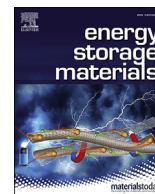




Contents lists available at ScienceDirect

Energy Storage Materials

journal homepage: www.elsevier.com/locate/ensm

Rechargeable Mg metal batteries enabled by a protection layer formed *in vivo*

Jiahua Zhang^a, Xuze Guan^a, Ruijing Lv^a, Donghong Wang^{b,**}, Ping Liu^c, Jiayan Luo^{a,*}^a Key Laboratory for Green Chemical Technology of Ministry of Education, School of Chemical Engineering and Technology, Tianjin University & Collaborative Innovation Center of Chemical Science and Engineering (Tianjin) Tianjin, 300072, China^b Shanghai Key Laboratory for High Temperature Materials and Precision Forming, School of Materials Science and Engineering, Shanghai Jiao Tong University, Shanghai, 200240, China^c Department of NanoEngineering, University of California San Diego, La Jolla, CA, 92093, USA

ARTICLE INFO

Keywords:

Protection layer
Mg metal anodes
Passivation
Additive
In vivo

ABSTRACT

The rise of rechargeable Mg batteries, a candidate for replacing lithium-ion batteries, is constrained by the electrolytes severely. Unfortunately, the Mg anode usually forms a blocking layer to impede the penetration of divalent Mg^{2+} in traditional electrolytes. Here, we demonstrate a protection layer formed *in vivo* on the surface of Mg metal anodes by adding $GeCl_4$ into ether electrolyte, successfully preserving structure stability and showing a low overpotential even at high current density of 10 mA cm^{-2} . Due to the excess additives in electrolyte, self-repair effect of the protection layer emerges over electrochemical cycling. Significantly, full cells with Mg metal anodes paired with both TiS_2 and Ti_3C_2 cathodes in $GeCl_4$ -containing ether electrolyte are also presented. Our work paves a new way towards rational design of self-repair protection layer via a facile chemistry route in simple Mg salt electrolyte system.

1. Introduction

The challenges that current rechargeable battery systems face are high energy density, material sustainability and safety [1]. Due to the limited capacity, commercial lithium-ion batteries fail in meeting the ever-growing energy density demand with the development of portable electronic devices and electric vehicles [2]. As one of the most potential alternatives, rechargeable Mg metal batteries (RMBs) have received extensive attention in virtue of some fascinating features of metallic magnesium. Mg metal anodes have natural superiority of high theoretical volumetric capacity (3833 mAh cm^{-3}), abundance in earth's crust, and low redox potential (-2.37 V versus the standard hydrogen electrode). Moreover, Mg metal anodes possess the characteristics of environmentally friendly and relatively low activity [3]. In most cases unlike metallic lithium, magnesium will not form dendrites during repeated deposition/dissolution process [4]. Therefore, it is of great possibility to promote safety of batteries with high energy density when using metallic magnesium as the anode. However, there are still some challenges that hinder the commercial applications of RMBs.

One of the pivotal obstacles is the lack of an ideal electrolyte that can

effectively transfer Mg^{2+} . Great efforts have been devoted to developing suitable electrolytes capable of reversible plating/stripping of Mg. A groundbreaking work from Nelson's group demonstrated that soluble Grignard reagent ($RMgX$, R is alkyl or aryl, X is halogen) dissolved in ether solvent electrolytes can achieve reversible deposition/dissolution of magnesium. However, this electrolyte showed poor anodic stability and quite low ionic conductivity [5]. Gregory and coworkers subsequently found that adding strong Lewis acid $AlCl_3$ into Grignard reagent could effectively enhance the interphase stability between electrolyte and anode [6]. A breakthrough in prototype systems for non-aqueous rechargeable magnesium batteries was first demonstrated by Aurbach's group in 2000 with Mg organohaloaluminate salts in ether solvents based on Lewis acid-base theory [7]. Afterwards, various Grignard reagent-based and organoborate-based electrolytes have been proposed to allow stable and fast Mg^{2+} conducting while avoiding the generation of blocking layer [8]. Nevertheless, these complex electrolytes are difficult to synthesize and highly sensitive to air and moisture, and usually toxic and costly. Moreover, these electrolytes can be compatible with few types of cathodes due to their poor anodic stability and unsatisfactory stability against current collector corrosion. Apart from electrolytes containing

* Corresponding author.

** Corresponding author.

E-mail addresses: wangdh2009@sjtu.edu.cn (D. Wang), jluo@tju.edu.cn (J. Luo).<https://doi.org/10.1016/j.ensm.2019.11.012>

Received 20 October 2019; Received in revised form 4 November 2019; Accepted 5 November 2019

Available online xxx

2405-8297/© 2019 Published by Elsevier B.V.

heavy organometallic magnesium complex, using simple Mg salt (e.g., $\text{Mg}(\text{PF}_6)_2$, $\text{Mg}(\text{BF}_4)_2$, $\text{Mg}(\text{TFSI})_2$, etc.) is another promising strategy to realize reversibility of RMBs. Different from the solid electrolyte interface (SEI) transporting Li^+ in Li batteries, a passivation layer hindering Mg^{2+} conduct would be formed induced by the decomposition of electrolyte components or parasitic reactions between electrolytes and anodes [9]. $\text{Mg}(\text{TFSI})_2$, one of the very few Mg salts possessing reasonable solubility in ether solvents, is highly resistant to oxidation and provides a wide operating voltage range. Unfortunately, $\text{Mg}(\text{TFSI})_2$ -based electrolytes usually show a poor electrochemical performance as a result of the decomposition of Mg salt forming a MgF_2 -rich blocking layer, which impedes reversible Mg plating/stripping (Fig. 1a) [9b,10]. Recently, Ban and co-workers made an important breakthrough in the development of a PAN-based protection layer engineered on the Mg anode surface as an artificial Mg^{2+} -conducting interphase in $\text{Mg}(\text{TFSI})_2/\text{PC}$ electrolyte to realize reversible Mg plating/stripping [11]. Besides facilitating Mg^{2+} conducting, an ideal protection layer should maintain structure and component stability during long-term cycling. However, it should be noted that high current density and accidental damage often lead to a loose structure of the artificial film. As a result, the protection layer may crack or even partially peel off so that the bare region would be passivated again due to the direct contact between Mg anode and electrolyte (Fig. 1b).

Herein, we propose a facile surface chemistry approach to accomplish a Ge-based protection layer *in vivo* on the surface of Mg metal by adding GeCl_4 into $\text{Mg}(\text{TFSI})_2/\text{DME}$ electrolyte. The Ge-based protection layer provides a pathway for rapid Mg^{2+} transport and meanwhile prevents the formation of the passivation film on the Mg anode surface. Electrochemical performance shows that a low and stable overpotential was exhibited during plating/stripping process in GeCl_4 -containing ether electrolyte, even at high current density of 10 mA cm^{-2} . On account of excess additives in electrolyte, a self-repair process would occur when the artificial protection film ruptures abruptly (Fig. 1c). Furthermore, a steady cycling performance is illustrated in both $\text{Mg}|\text{TiS}_2$ and $\text{Mg}|\text{Ti}_3\text{C}_2$ full cells with GeCl_4 -containing ether electrolyte.

Theoretically, Ge^{4+} in modified electrolyte can automatically replace the surface atoms of metallic Mg via a facile galvanic replacement reaction because Ge has a more positive equilibrium potential than Mg ($E_{\text{Ge}^{4+}/\text{Ge}}^0 = 0.124 \text{ V}$ versus SHE, $E_{\text{Mg}^{2+}/\text{Mg}}^0 = -2.37 \text{ V}$ versus SHE).



The relative Gibbs free energy ($\Delta G = -nFE$) indicates a spontaneous formation of Ge on Mg metal surface. DFT calculations show that Ge metal provides a quite low migration for Mg^{2+} diffusion, thus the as-prepared Ge-based protection layer favors the transport of Mg^{2+} in the bulk phase [12]. To substantiate the hypothesis, symmetric Mg cells in

GeCl_4 -containing electrolytes were assembled and rested for 48 h, after which the cells were disassembled to analyze the nature of the Mg anode surface. Obviously, optical photos indicate that a dark grey layer is generated *in vivo* on the Mg metal surface using the electrolyte with 0.4 M GeCl_4 , while the electrode in blank electrolyte is almost unchanged (Fig. S1). For Mg anodes exposed to the electrolyte containing GeCl_4 , Raman spectra show two obvious peaks centered at 200 and 300 cm^{-1} , assigned to Ge, GeO_x peaks, respectively. However, no sharp Raman-active peaks appear in the frequency range of $100\text{--}1400 \text{ cm}^{-1}$ for electrode in blank electrolyte (Fig. S2). As can be seen from the energy dispersive X-ray spectroscopy (EDX) mapping, Mg, Ge and few Cl elements are distributed uniformly on the surface layer (Fig. 2a–d). The consistency of above observations reveals that Ge-rich artificial layer can be formed *in vivo* on Mg metal surface by direct immersing the electrode in GeCl_4 -containing ether electrolyte.

SEM and X-ray photoelectron spectroscopy (XPS) characterization were performed to acquire the composition of the Ge-based protection layer and further investigate the stability upon cycling. Top-view SEM images show that an uneven surface layer is formed on Mg anode in 0.4 M GeCl_4 -containing electrolyte after resting for 48 h, while the surface pattern layer maintains largely unchanged after 30 cycles (Fig. 2e, f). As exhibited in Fig. 2g, high-resolution XPS spectra of Ge 3d showed that the major Ge-containing components on the surface are Ge, GeO and GeO_2 [13]. The XPS spectra of Mg 1s can be fitted into three Gauss peaks centered at 1303.3 , 1304.2 , and 1305.1 eV , which are assigned to Mg, MgO, and MgCl_2 , respectively [14]. The C 1s spectrum shows several split peaks centered at 284.8 , 286.2 , 287.7 , and 289.4 eV , respectively, corresponding to C–C, C–O, C=O, and CO_3^{2-} functional groups [15]. Notably, the composition of electrode surface layer after 30 cycles is quite similar with that in the fresh cell (Fig. 2h, Fig. S3), indicating the Ge-based protection layer maintains compositionally stable over cycling and no passivation layer is formed during repeated plating/stripping process.

Galvanostatic charge/discharge measurement was carried out in symmetric Mg cells to validate the Mg^{2+} transport property of the Ge-based protection layer on Mg anodes. A capacity of $0.005 \text{ mAh cm}^{-2}$ at current density of 0.01 mA cm^{-2} was continuously cycling in each charge/discharge cycle. As displayed in Fig. 3a, the symmetric cells with modified electrolyte show an exceptionally stable voltage profile with a quite low overpotential ($\sim 250 \text{ mV}$) over 1000 h at current density of 0.02 mA cm^{-2} , possibly attributed to unhindered ionic diffusion in the *in vivo* formed Mg^{2+} -conducting film. On the contrary, the Mg anode in blank electrolyte exhibits a high overpotential with reduced lifetime, indicating that the anode undergoes severe passivation during cycling. The passivation layer quickly shuts off the pathway of Mg^{2+} , leading to an irreversible plating/stripping behavior. Similar galvanostatic plating/

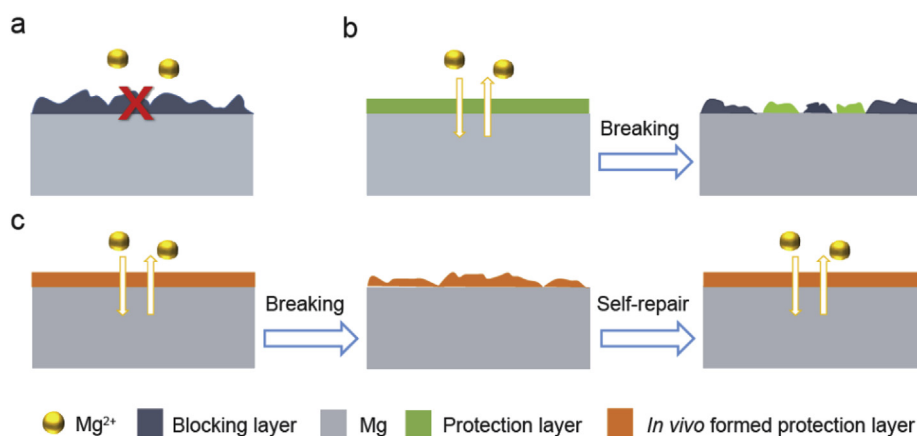


Fig. 1. Schematic diagrams showing the (a) passivation layer in blank electrolyte, (b) breaking process for protection layer and (c) breaking and self-repair process for *in vivo*-formed protection layer during Mg plating/stripping in conventional organic electrolyte.

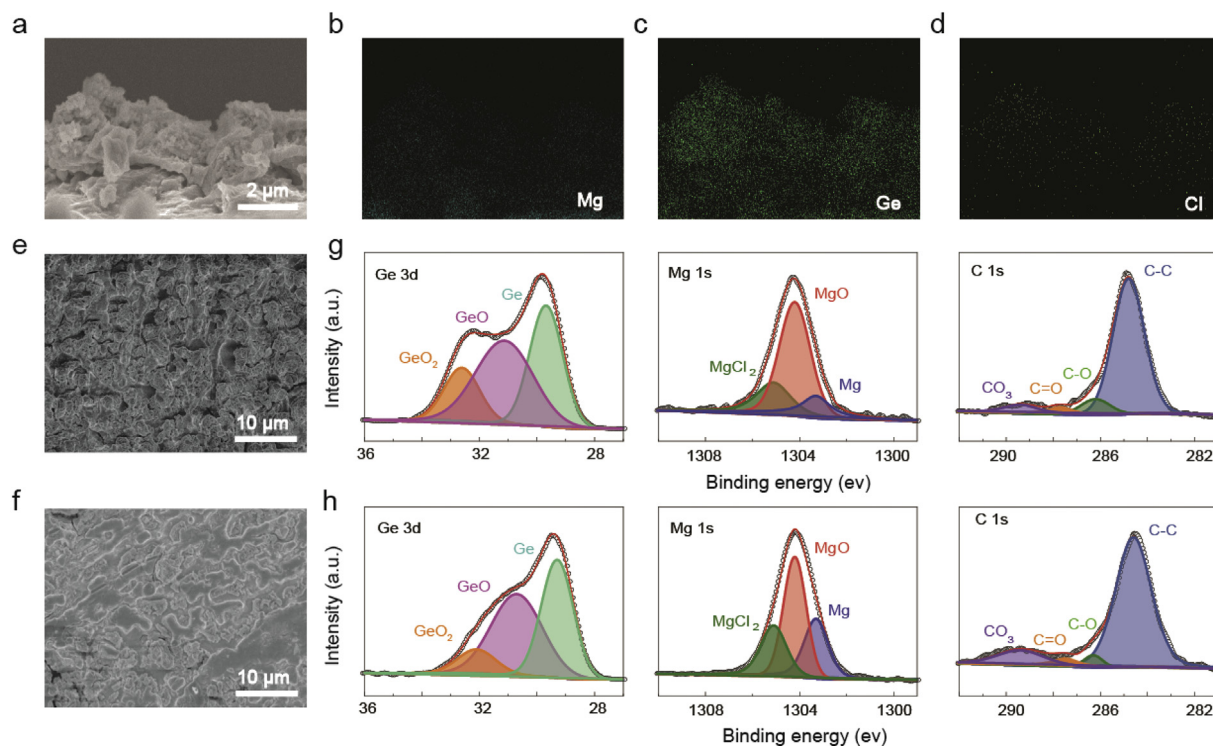


Fig. 2. Characterization of the Ge-based protection layer. (a) Cross-section SEM image (b–d) the corresponding EDX mapping analysis of the Ge-based protection layer. Top-view SEM image of Mg metal electrode (e) in fresh cell and (f) after 30 cycles. XPS of Mg metal electrode (g) in fresh cell and (h) after 30 cycles using 0.4 M GeCl_4 in 0.5 M $\text{Mg}(\text{TFSI})_2/\text{DME}$ electrolyte.

stripping experiments in Mg symmetric cells were performed under extremely high current density of 10 mA cm^{-2} and capacity of 5 mAh cm^{-2} . Fig. 3b showed that the cells in GeCl_4 -containing electrolyte exhibit remarkable reversibility without pronounced voltage fluctuation over 350 h. As a comparison, symmetric Mg cells with the electrolyte containing various different concentrations of GeCl_4 were also examined (Fig. S5).

XPS analysis is conducted to further acquire the stability of the anode surface upon cycling (Fig. 3c). After cycling, the ratios of C 1s to Mg 1s ($R_{\text{C:Mg}}=0.36$) and F 1s to Mg 1s ($R_{\text{F:Mg}}=0.31$) of the anode surface in GeCl_4 -containing electrolyte are far less than that in blank electrolyte ($R_{\text{C:Mg}}=0.80$ and $R_{\text{F:Mg}}=0.54$). Note that the Mg anode surface in GeCl_4 -containing electrolyte is enriched with Ge. The actual C/Mg and F/Mg ratio disparity should be much larger. This demonstrates that the parasitic reactions between TFSI and Mg anode and the decomposition of electrolytes have been restricted substantially due to *in-vivo* formed Ge-based protection layer. It is reported that the addition of MgCl_2 can effectively improve the reversibility of Mg deposition and stripping [9b, 9d, 16]. To further exclude the effect of Cl^- in electrolyte, an electrolyte containing MgCl_2 with equivalent amount of Cl^- in GeCl_4 -containing electrolyte was formulated. As depicted in Fig. S6, a more stable voltage profile with dramatic lowering of overpotential is attained in GeCl_4 -containing electrolyte, implying that the Ge-based artificial protection layer formed on Mg surface plays a significant role in enhancing the cycle life of the symmetric cells.

Furthermore, engraving-reassembling experiment was carried out to verify the self-repair property of Ge-based protection film. After 30 cycles at 2 mA cm^{-2} , the symmetric cell with modified electrolyte was disassembled. Then a Z-shaped scar was engraved on the surface of the electrode and SEM images clearly reveal the boundary lines of the gap (Fig. 4b). These gaps were $\sim 1.5 \text{ mm}$ in width and $\sim 4 \text{ mm}$ in length following the model (Fig. S7). EDX mapping further confirms the components of the exposed gap are almost Mg (Fig. S8). Then the engraved electrode was reassembled under the same assembly condition (using

previous electrolyte). As shown in Fig. 4a, the reassembled cell undergoes a temporary fluctuation during the initial cycles and exhibits reasonably stable voltage profile once the protection film re-formed. The result suggests that an *in-vivo* self-repair process would occur when the protection film cracks unexpectedly or fails at the strains encountered upon cycling [17], benefitted from the excess additive in electrolytes and fast galvanic replacement reaction between GeCl_4 and metallic Mg. After a few cycles, the Z-shaped scar disappears and the engraved anode surface turns to grey tarnish (Fig. 4c). SEM images and EDX mapping further demonstrate that a new Ge-rich artificial layer forms on the fresh Mg surface, which is consistent with the expectation of self-repair nature and the electrochemical results.

To assess the location of plated Mg, the symmetric Mg cell with modified electrolyte was disassembled after plating 3 mAh cm^{-2} of Mg. Fig. 5a, b shows cross-section view of the protected anode after deposition in secondary electron detection mode and backscattered mode, respectively. The deposited Mg layer appears bright in secondary electron detection mode, but dark in backscattered mode, which verifies that metallic Mg plates underneath the protection film. Similar to ion-conducting artificial layer for Li metal anode [18], the insulating components (such as Mg-Cl and Ge-Cl) in the artificial layer inhibit the deposition of Mg on the surface and generate a potential gradient to drive Mg^{2+} flow through the layer. As a proof of concept, full cells were assembled to prove the efficacy of the Ge-based artificial Mg^{2+} -conducting layer. TiS_2 , a well-established intercalation cathode [19] was coupled with Mg metal anode in modified electrolyte or blank electrolyte. As displayed in Fig. 5c, owing to the Ge-based protection layer formed *in vivo*, the cell delivers significantly enhanced reversibility and cycling stability in modified electrolyte, with a reversible capacity of 87.8 mAh g^{-1} over 30 cycles at a rate of 10 mA g^{-1} (Fig. S11). As a comparison, rapid capacity fading is observed in blank ether electrolyte system and the capacity drops to zero only after 5 cycles (Fig. 5c, Fig. S12). The severe capacity decay is mainly attributed to the formation of passivation film from the decomposition of TFSI, which impedes Mg^{2+} diffusion.

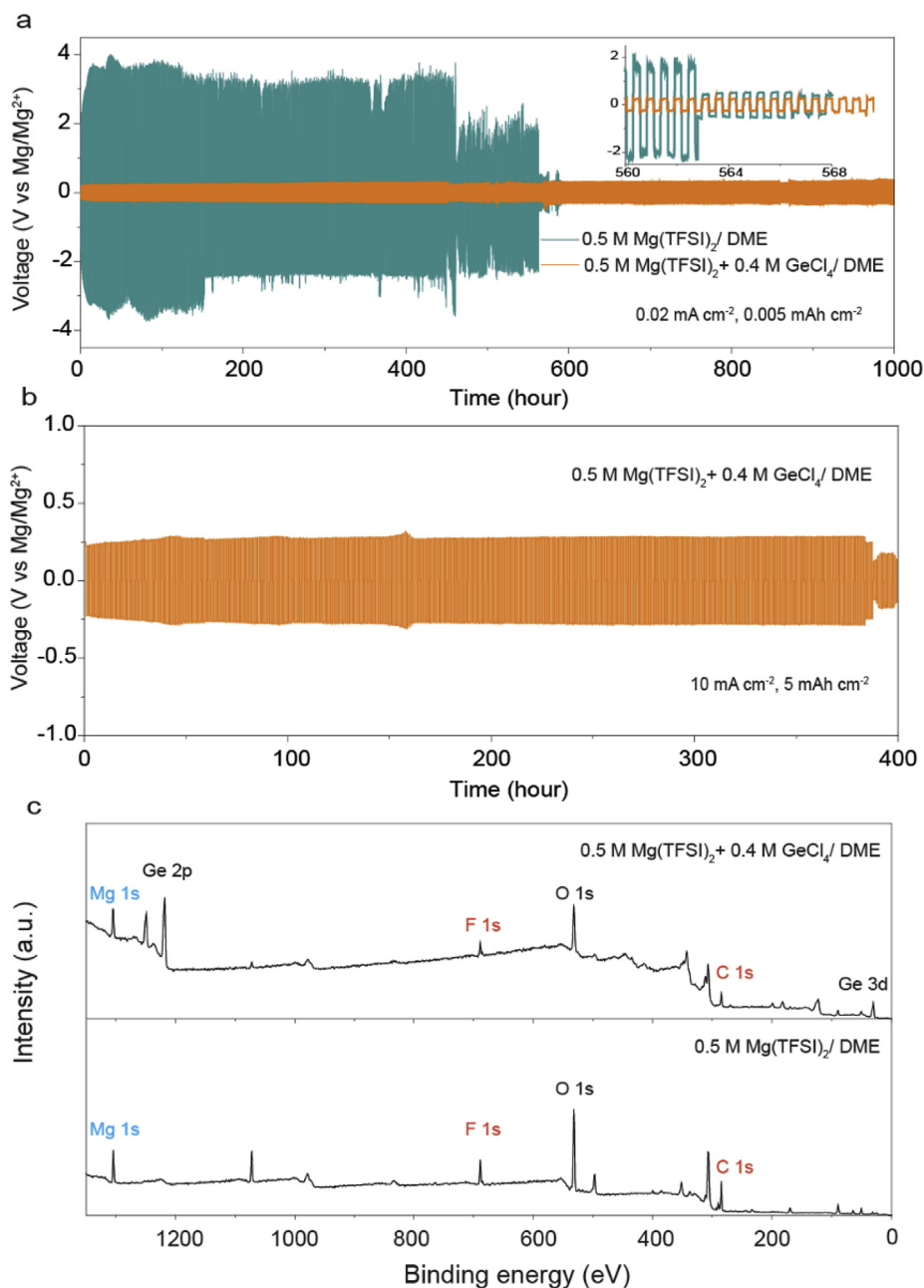


Fig. 3. Symmetric cell performance. Voltage responses of symmetric Mg cells under repeated polarization from (a) 1/4 h charge/discharge cycling at 0.02 mA cm^{-2} , (b) 1/2 h charge/discharge cycling at 10 mA cm^{-2} . (c) The XPS survey of surface layer for symmetric Mg cells under 1/4 h discharge and 1/4 h charge cycles at 0.2 mA cm^{-2} in different electrolytes.

Further interrogation of the artificial protection film was carried out in full cells with an optimized cathode Ti_3C_2 MXene material (Figs. S9 and 10) [20]. It has been reported that preintercalating cationic surfactant CTAC into MXene membrane can significantly accelerate multivalent Mg^{2+} insertion kinetics [21]. Predictably, with self-standing Ti_3C_2 @CTAC cathode, the cells in modified electrolyte deliver excellent stability with a high discharge capacity of $\sim 100 \text{ mAh g}^{-1}$ even at 50 mA g^{-1} (Fig. 5d, Fig. S13). Nevertheless, the discharge capacity of cells in blank ether electrolyte drops rapidly to zero with an increased overpotential value (Fig. 5d, Fig. S14). Furthermore, the full cells with electrolyte only containing 0.4 M GeCl_4 were performed (Fig. S15). The contribution of specific capacity is almost negligible compared to those cells using 0.5 M Mg(TFSI)_2 - 0.4 M GeCl_4 electrolyte, especially with Ti_3C_2 cathode. Dozens of compounds are expected to react with metallic Mg, yielding an artificial film composed of Mg^{2+} -conducting metals or alloys. We also

prove that SbCl_3 additive in $\text{Mg(TFSI)}_2/\text{DME}$ electrolyte is effective to prevent the Mg anode from passivation and enhance diffusion kinetics at the surface (Fig. S16).

In summary, we have proposed a Ge-based protection layer formed *in vivo* on Mg metal anode via a simple galvanic replacement reaction, providing a Mg^{2+} -conducting passage for Mg electroplating. The protection film not only prevents the formation of Mg^{2+} -blocking layers, but maintains compositionally invariable during long-term cycling. Meanwhile, the Ge-based artificial layer can effectively promote Mg^{2+} diffusion and the insulating components prevent Mg deposition on the surface. Notably, a self-repair behavior of the protection layer is observed when the film undergoes an unexpected break or uneven strain distribution upon cycling. Thus our strategy paves a new way towards rational surface modification of monovalent or multivalent metal anode in simple-salt-based organic electrolytes for rechargeable metal batteries.

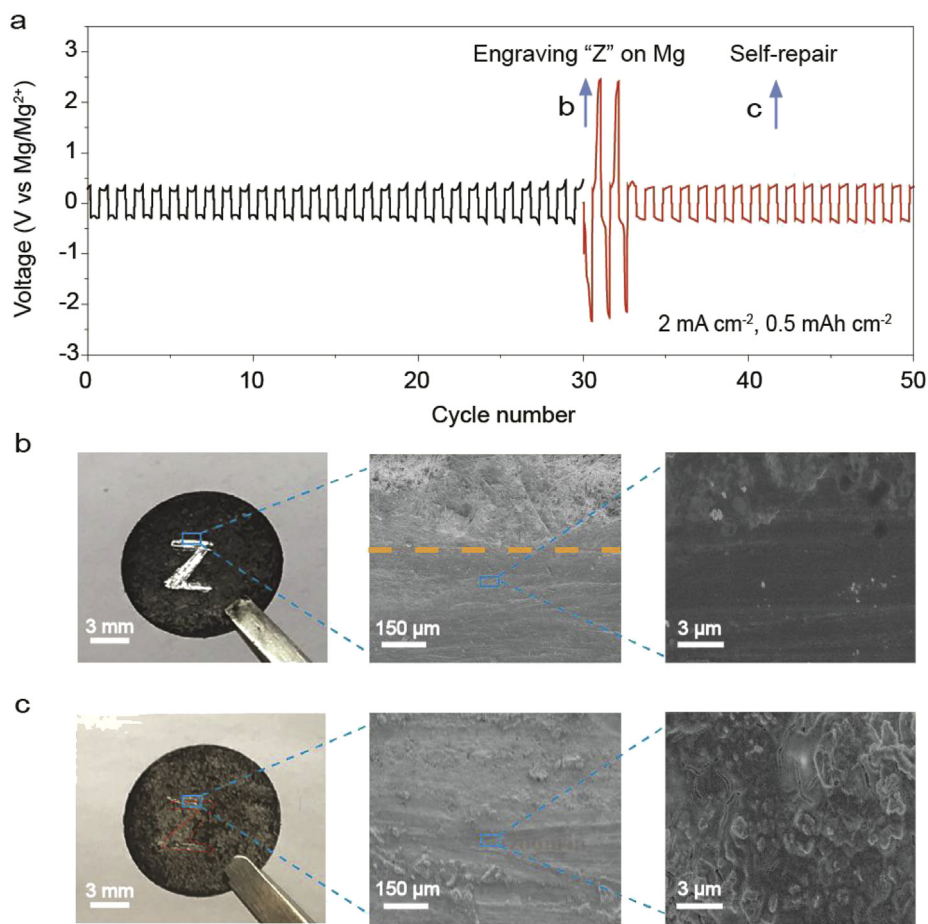


Fig. 4. Self-repair of Ge-based protection film. (a) Voltage response of symmetric Mg cells from 1/4 h charge/discharge cycling at current density of 2 mA cm^{-2} using 0.4 M GeCl_4 in $0.5 \text{ M Mg(TFSI)}_2/\text{DME}$. Optical and SEM images of (b) engraved "Z" on the protected anode surface at 30 cycles and (c) self-repair of the protected anode after 50 cycles.

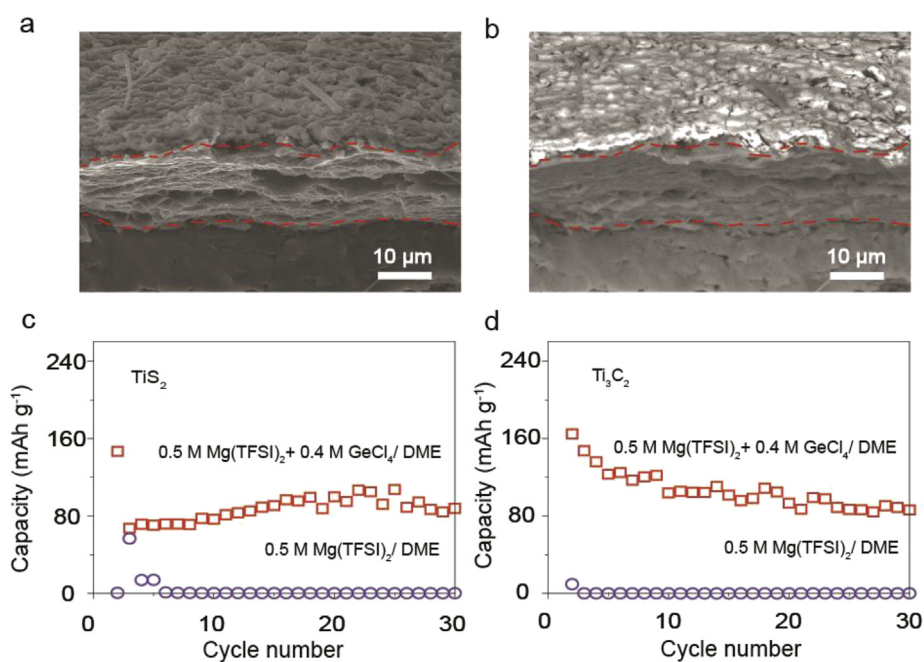


Fig. 5. Full cell performance. Cross-section SEM images of protected anode after 3 mAh cm^{-2} Mg plating using 0.4 M GeCl_4 in $0.5 \text{ M Mg(TFSI)}_2/\text{DME}$ electrolyte in symmetric Mg cell in (a) secondary electron mode and (b) backscattered mode. Cycling performance of (c) Mg/TiS₂ and (d) Mg/Ti₃C₂ full cell.

Declaration of competing interest

The authors declare that they have no known competing financial interests or personal relationships that could have appeared to influence the work reported in this paper.

Acknowledgement

J. Z. and X. G. contributed equally to this work. The authors appreciate support from National Natural Science Foundation of China (Grant Nos. 51872196), Natural Science Foundation of Tianjin, China (Grant Nos. 17JCJQC44100).

Appendix A. Supplementary data

Supplementary data to this article can be found online at <https://doi.org/10.1016/j.ensm.2019.11.012>.

References

- [1] a) M. Armand, J.-M. Tarascon, *Nature* 451 (2008) 652;
b) H.D. Yoo, E. Markevich, G. Salitra, D. Sharon, D. Aurbach, *Mater. Today* 17 (2014) 110–121.
- [2] a) J.M. Tarascon, M. Armand, *Nature* 414 (2001) 359–367;
b) R. Schmich, R. Wagner, G. Hörpel, T. Placke, M. Winter, *Nat. Energy* 3 (2018) 267–278.
- [3] a) H.D. Yoo, I. Shterenberg, Y. Gofer, G. Gershinshy, N. Pour, D. Aurbach, *Energy Environ. Sci.* 6 (2013) 2265;
b) Y.-s. Guo, F. Zhang, J. Yang, F.-f. Wang, Y. NuLi, S.-i. Hirano, *Energy Environ. Sci.* 5 (2012) 9100;
c) T.J. Carter, R. Mohtadi, T.S. Arthur, F. Mizuno, R. Zhang, S. Shirai, J.W. Kampf, *Angew. Chem. Int. Ed.* 53 (2014) 3173–3177;
d) R.E. Doe, R. Han, J. Hwang, A.J. Gmitter, I. Shterenberg, H.D. Yoo, N. Pour, D. Aurbach, *Chem. Commun.* 50 (2014) 243–245.
- [4] C. Ling, D. Banerjee, M. Matsui, *Electrochim. Acta* 76 (2012) 270–274.
- [5] J.M. Nelson, W.V. Evans, *J. Am. Chem. Soc.* 39 (1917) 82–83.
- [6] T.D. Gregory, R.J. Hoffman, R.C. Winterton, *J. Electrochem. Soc.* 137 (1990) 775–780.
- [7] D. Aurbach, Z. Lu, A. Schechter, Y. Gofer, H. Gizbar, R. Turgeman, Y. Cohen, M. Moshkovich, E. Levi, *Nature* 407 (2000) 724.
- [8] a) N. Pour, Y. Gofer, D.T. Major, D. Aurbach, *J. Am. Chem. Soc.* 133 (2011) 6270–6278;
b) A. Du, Z. Zhang, H. Qu, Z. Cui, L. Qiao, L. Wang, J. Chai, T. Lu, S. Dong, T. Dong, H. Xu, X. Zhou, G. Cui, *Energy Environ. Sci.* 10 (2017) 2616–2625;
c) M. Salama, I. Shterenberg, L.J.W. Shimon, K. Keinan-Adamsky, M. Afri, Y. Gofer, D. Aurbach, *J. Phys. Chem. C* 121 (2017) 24909–24918.
- [9] a) Z. Lu, A. Schechter, M. Moshkovich, D. Aurbach, *J. Electroanal. Chem.* 466 (1999) 203–217;
b) I. Shterenberg, M. Salama, H.D. Yoo, Y. Gofer, J.-B. Park, Y.-K. Sun, D. Aurbach, *J. Electrochem. Soc.* 162 (2015) A7118–A7128;
c) S. Terada, T. Mandai, S. Suzuki, S. Tsuzuki, K. Watanabe, Y. Kamei, K. Ueno, K. Dokko, M. Watanabe, *J. Phys. Chem. C* 120 (2016) 1353–1365;
d) J.G. Connell, B. Genorio, P.P. Lopes, D. Strmcnik, V.R. Stamenkovic, N.M. Markovic, *Chem. Mater.* 28 (2016) 8268–8277;
e) N.N. Rajput, X. Qu, N. Sa, A.K. Burrell, K.A. Persson, *J. Am. Chem. Soc.* 137 (2015) 3411–3420.
- [10] M. Salama, I. Shterenberg, H. Gizbar, N.N. Eliaz, M. Kosa, K. Keinan-Adamsky, M. Afri, L.J.W. Shimon, H.E. Gottlieb, D.T. Major, Y. Gofer, D. Aurbach, *J. Phys. Chem. C* 120 (2016) 19586–19594.
- [11] S.B. Son, T. Gao, S.P. Harvey, K.X. Steirer, A. Stokes, A. Norman, C. Wang, A. Cresce, K. Xu, C. Ban, *Nat. Chem.* 10 (2018) 532–539.
- [12] O.I. Malyi, T.L. Tan, S. Manzhos, *J. Power Sources* 233 (2013) 341–345.
- [13] K. Prabhakaran, T. Ogino, *Surf. Sci.* 325 (1995) 263–271.
- [14] a) J.S. Corneille, J.-W. He, D.W. Goodman, *Surf. Sci.* 306 (1994) 269–278;
b) H. Seyama, M. Soma, *J. Chem. Soc. Faraday Trans. I* 81 (1985) 485–495.
- [15] K.P. Yao, D.G. Kwabi, R.A. Quinlan, A.N. Mansour, A. Grimaud, Y.-L. Lee, Y.-C. Lu, Y. Shao-Horn, *J. Electrochem. Soc.* 160 (2013) A824–A831.
- [16] Y. Cheng, R.M. Stolley, K.S. Han, Y. Shao, B.W. Arey, N.M. Washon, K.T. Mueller, M.L. Helm, V.L. Sprenkle, J. Liu, G. Li, *Phys. Chem. Chem. Phys.* 17 (2015) 13307–13314.
- [17] a) M.D. Tikekar, S. Choudhury, Z. Tu, L.A. Archer, *Nat. Energy* 1 (2016) 16114;
b) M.N. Obrovac, V.L. Chevrier, *Chem. Rev.* 114 (2014) 11444–11502;
c) J. Li, R. Lewis, J. Dahn, *Electrochem. Solid State Lett.* 10 (2007) A17–A20.
- [18] a) X. Liang, Q. Pang, I.R. Kocchetkov, M.S. Sempere, H. Huang, X. Sun, L.F. Nazar, *Nat. Energy* 2 (2017) 17119;
b) K. Liao, S. Wu, X. Mu, Q. Lu, M. Han, P. He, Z. Shao, H. Zhou, *Adv. Mater.* 30 (2018) 1705711;
c) Z. Tu, S. Choudhury, M.J. Zachman, S. Wei, K. Zhang, L.F. Kourkoutis, L.A. Archer, *Nat. Energy* 3 (2018) 310–316;
d) Q. Pang, X. Liang, I.R. Kocchetkov, P. Hartmann, L.F. Nazar, *Angew. Chem.* 130 (2018) 9943–9946.
- [19] M.S. Whittingham, *Science* 192 (1976) 1126–1127.
- [20] a) M.R. Lukatskaya, O. Mashtalir, C.E. Ren, Y. Dall'Agnese, P. Rozier, P.L. Taberna, M. Naguib, P. Simon, M.W. Barsoum, Y. Gogotsi, *Science* 341 (2013) 1502–1505;
b) M. Ghidui, M.R. Lukatskaya, M.Q. Zhao, Y. Gogotsi, M.W. Barsoum, *Nature* 516 (2014) 78–81;
c) B. Anasori, M.R. Lukatskaya, Y. Gogotsi, *Nat. Rev. Mater.* 2 (2017) 16098.
- [21] M. Xu, S. Lei, J. Qi, Q. Dou, L. Liu, Y. Lu, Q. Huang, S. Shi, X. Yan, *ACS Nano* 12 (2018) 3733–3740.